

xRFM: Accurate, scalable, and interpretable feature learning models for tabular data

Daniel Beaglehole
 Computer Science and Engineering
 Halıcıoğlu Data Science Institute
 UC San Diego
 dbeaglehole@ucsd.edu

Adityanarayanan Radhakrishnan
 MIT Mathematics
 Broad Institute of MIT and Harvard
 aradha@mit.edu

David Holzmüller
 INRIA Paris
 Ecole Normale Supérieure
 PSL University
 david.holzmuller at inria.fr

Mikhail Belkin
 Halıcıoğlu Data Science Institute
 UC San Diego
 mbelkin@ucsd.edu

Abstract

Inference from tabular data, collections of continuous and categorical variables organized into matrices, is a foundation for modern technology and science. Yet, in contrast to the explosive changes in the rest of AI, the best practice for these predictive tasks has been relatively unchanged and is still primarily based on variations of Gradient Boosted Decision Trees (GBDTs). Very recently, there has been renewed interest in developing state-of-the-art methods for tabular data based on recent developments in neural networks and feature learning methods. In this work, we introduce xRFM, an algorithm that combines feature learning kernel machines with a tree structure to both adapt to the local structure of the data and scale to essentially unlimited amounts of training data.

We show that compared to 31 other methods, including recently introduced tabular foundation models (TabPFNv2) and GBDTs, xRFM achieves best performance across 100 regression datasets and is competitive to the best methods across 200 classification datasets outperforming GBDTs. Additionally, xRFM provides interpretability natively through the Average Gradient Outer Product. Code for xRFM (following a scikit-learn-style API) is available at: <https://github.com/dmbeaglehole/xRFM>.

1 Introduction

Tabular data – collections of continuous and categorical variables organized into matrices – underlies all aspects of modern commerce and science from airplane engines to biology labs to bagel shops. Yet, while Machine Learning and AI for language and vision have seen unprecedented progress, the primary methodologies of prediction from tabular data have been relatively static, dominated by variations of Gradient Boosted Decision Trees (GBDTs), such as XGBoost [7]. Nevertheless, hundreds of tabular datasets have been assembled to form extensive regression and classification benchmarks [11, 12, 16, 35, 37], and, recently, there has been renewed interest in building state-of-the-art predictive models for tabular data [15, 18, 19]. Notably, given the remarkable effectiveness of large, “foundation” models for text, there has been much excitement in developing similar models on tabular data, and recent effort has led to the development of TabPFN-v2, a foundation model for tabular data appearing in Nature [18]. Yet, despite this progress, tabular data still remains an active area for model development and building scalable, effective, and interpretable machine learning models in this domain remains an open challenge.

In this work, we introduce xRFM, a tabular predictive model that combines recent advances in feature learning kernel machines with an adaptive tree structure, making it effective, scalable, and interpretable. xRFM builds upon the Recursive Feature Machine (RFM) algorithm from [27], which enabled *feature learning* (a form of supervised dimensionality reduction) in general machine learning models. xRFM works as follows – given training data, it first builds a binary tree structure to split data into subsets based on features

relevant for prediction within each split. When splits reach a certain size (of $\leq C$ data samples), we train a *leaf* RFM (a hyper-parameter and compute optimized version of RFM from [28]).

There are two important consequences of using a tree structure in conjunction with leaf RFMs. The first is that it enables *local feature learning*, meaning that xRFM can learn different features for different subsets of the data. This property is crucial for tackling hierarchical structure in tabular data (for example, one subset of features may become relevant when a specific feature takes on high value while another subset of features is relevant when the same feature takes low values). The second consequence is that it enables xRFM to scale log-linearly in the number of samples ($O(n \log n)$ given n samples) during training and logarithmically ($O(\log n)$) during inference. As such, the inference time of xRFM is comparable to that of tree-based models.

In practice, we show xRFM has the best performance across 100 tabular regression tasks and is competitive with state-of-the-art on 200 tabular classification tasks from the TALENT benchmark [37]. In particular, xRFM outperforms 31 other methods on these regression tasks including the GBDT and neural network variations mentioned in the opening paragraph. We show that xRFM achieves similar results on the largest datasets from the meta-test benchmark, where directly solving standard kernel machines becomes intractable on standard GPUs [19]. An additional benefit of xRFM is that it natively provides interpretability by exposing features learned and used for prediction. In particular, each leaf RFM learns features through a mathematical object known as the Average Gradient Outer Product (AGOP), whose diagonal indicates coordinates relevant for prediction and whose top eigenvectors indicate directions in data most relevant for prediction. Using examples of xRFM trained on synthetic and real data from TALENT, we show how AGOP matrices at each leaf RFM shed light on features relevant for prediction, including cases when leaf RFMs learn different features for different splits of data.

To summarize, xRFM combines feature learning kernel methods with adaptive data partitioning using the AGOP. It is a fast, effective, and interpretable model on tabular data at all scales.

2 Preliminaries

We begin with a review of kernel machines and kernel-RFM, which we use to build xRFM.

2.1 Kernel machines

A kernel machine is a non-parametric machine learning model [3, 31]. The idea behind kernel machines is that one can train a nonlinear predictive model by first transforming input data with a fixed, nonlinear feature map and then performing linear regression on the transformed data. Kernel machines make this procedure computationally tractable even for infinite dimensional feature maps by using kernel functions (inner products of feature mapped data). We describe kernel machines in the context of supervised learning below. Let $X \in \mathbb{R}^{n \times d}$ denote training inputs with $x^{(i)T}$ denoting the example in the i^{th} row of X for $i \in [n]$ and $y \in \mathbb{R}^{n \times c}$ denote training labels. Let $K : \mathbb{R}^d \times \mathbb{R}^d \rightarrow \mathbb{R}$ denote a kernel function (a positive semi-definite, symmetric function). Given a regularization parameter $\lambda \geq 0$, a kernel machine trained on the data (X, y) is a predictor, $\hat{f} : \mathbb{R}^d \rightarrow \mathbb{R}^c$, of the form:

$$\hat{f}(x) = K(x, X)\alpha \quad ; \quad \alpha = (K(X, X) + \lambda I)^{-1}y ; \quad (1)$$

where the notation $K(x, X) \in \mathbb{R}^{1 \times n}$ denotes an n -dimensional row vector with $K(x, X)_i = K(x, x^{(i)})$ and $K(X, X) \in \mathbb{R}^{n \times n}$ denotes a matrix with $K(X, X)_{ij} = K(x^{(i)}, x^{(j)})$. Examples of kernel functions used in practice are the Gaussian kernel ($K(x, z) = \exp(-\|x - z\|_2^2/L^2)$) or the Laplace kernel ($K(x, z) = \exp(-\|x - z\|_2/L)$). The advantage of kernel functions is that the predictor admits a closed form solution, which can be computationally efficient to fit on datasets under 100k samples. The limitations of kernel machines are twofold: (1) the formulation in Eq. (1) does not scale well (it is super-quadratic in the number of samples) and (2) the choice of kernel is fixed independently of the input data. The former limitation is addressed by recent, pre-conditioned gradient descent methods for solving for α in Eq. (1) and methods that construct low-dimensional approximations of the kernel matrix. These include EigenPro [2, 22, 23], Falkon [29], and randomly pivoted Cholesky [8]. The latter limitation is addressed by procedures for adapting the kernel to the training data. We describe one such approach known as the kernel Recursive Feature Machine (kernel-RFM) below.

2.2 Recursive Feature Machines (RFMs)

The ability to learn task-relevant features from data is key to building effective predictors [1, 9, 13]. RFM, introduced in [27], is an algorithm that enables feature learning in general machine learning models through a mathematical object known as the Average Gradient Outer Product (AGOP). Given a predictive model $\hat{f} : \mathbb{R}^d \rightarrow \mathbb{R}$ and data $S = \{x^{(1)}, \dots, x^{(n)}\} \subset \mathbb{R}^d$, the AGOP is defined as

$$\text{AGOP}(\hat{f}, S) = \frac{1}{n} \sum_{i=1}^n \nabla \hat{f}(x^{(i)}) \nabla \hat{f}(x^{(i)})^T \in \mathbb{R}^{d \times d}, \quad (2)$$

where $\nabla \hat{f}(x^{(i)})$ denotes the gradient of \hat{f} at the point $x^{(i)}$. The AGOP is an estimate of the (un-centered) covariance of the gradients of \hat{f} and intuitively captures the subspace along which the predictor highly varies [20, 34]. The RFM algorithm involves iterating between training a predictive model and using the AGOP of the trained model to select features and linearly transform input data. As such, feature learning through RFM can be viewed as a form of “supervised” PCA.

In the particular case of kernel machines, which have no native mechanism for feature learning, RFM enables feature learning by adapting the kernel to the data. We describe the kernel-RFM algorithm below. Following the notation in the previous section, let (X, y) denote training inputs and labels, let K denote the kernel function, and λ denote the regularization parameter. Letting $M_1 = I$ and $c > 0$, kernel-RFM repeats the following two steps for T iterations:

$$\begin{aligned} \text{Step 1: } \hat{f}_t(x) &= K(M_t x, X M_t) \alpha_t \quad ; \quad \alpha_t = [K(X M_t, X M_t) + \lambda I]^{-1} y, \\ \text{Step 2: } M_{t+1} &= \left[\text{AGOP}(\hat{f}_t(M_t x), X) \right]^c. \end{aligned} \quad (3)$$

Typical choices of T and c in practice are $T \leq 10$ and $c \in \{\frac{1}{4}, \frac{1}{2}\}$ [4, 5, 24, 27]. (In practice, we return the f_t with best validation performance rather than returning \hat{f}_T .) When training labels, y , are multi-dimensional, we use the Jacobian of \hat{f} instead of the gradient in Step (2) (i.e., averaging the AGOP over output dimensions). Kernel-RFM is particularly effective at identifying low dimensional subspaces (or subsets of variables) relevant for prediction [28, 38], making it a useful interpretability tool, as we will show in Section 5.

3 xRFM algorithm overview

We now describe our algorithm xRFM, which consists of the following two components (Fig. 1):

- (1) An improved kernel-RFM, termed *leaf* RFM, that is trained on the subset of data;
- (2) A binary tree structure that splits the data into subsets, termed *leaves*, of a fixed maximum size (*leaf size*) that is independent of the number of training samples. Leaf RFMs are then trained using the data at each leaf. Splits involve stratifying data based on features relevant for prediction.

Together these components enable xRFM to perform local feature learning (learning different features on different subpopulations) and achieve $O(n \log n)$ training time as well as $O(\log n)$ inference time given n samples. We outline these two components in detail below.

3.1 Leaf RFM

Here, we describe the changes we made to the original kernel RFM algorithm from [27] to produce leaf RFMs. The kernel RFM model was primarily built using kernels that were invariant to orthonormal transformations of data (those where $K(x, z) = K(Ux, Uz)$ for any orthogonal matrix U). Examples include the Gaussian kernel of the form $K(x, z) = \exp(-L\|x - z\|_2^2)$ or the Laplace kernel of the form $K(x, z) = \exp(-L\|x - z\|_2)$. Such invariance does not effectively leverage a special property of tabular data – the fact that each coordinate can be independently meaningful. This property has been hypothesized as an explanation for the superior performance of tree-based models, which compose functions of individual coordinates, over traditional neural networks on tabular datasets [16]. To account for this special structure, we introduce the following modifications to kernel-RFM:

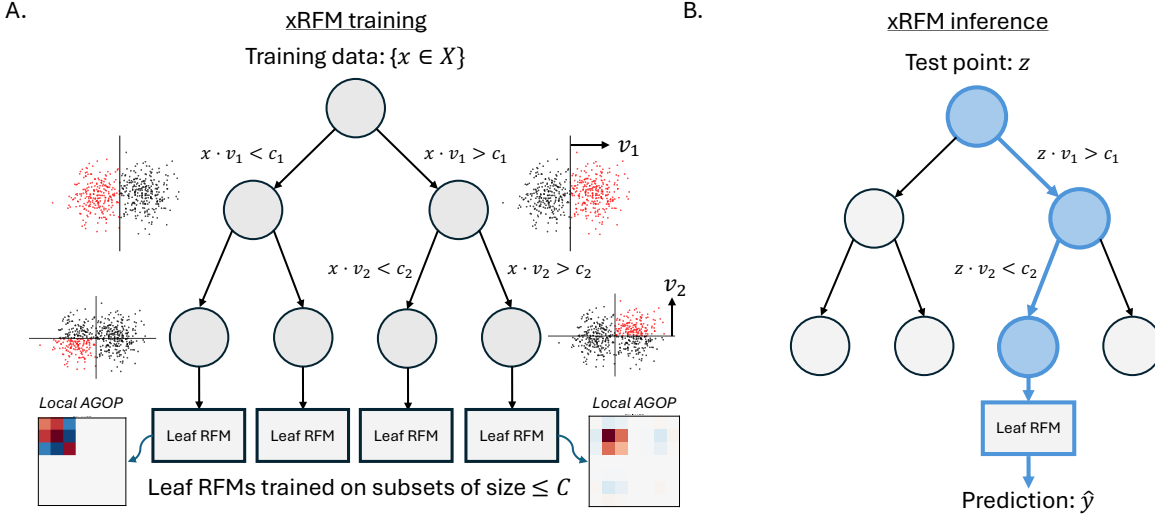


Figure 1: Overview of xRFM training and inference procedures. (A) xRFM is trained by splitting the data along the median projections (denoted c_1, c_2) onto computed split directions (denoted v_1, v_2). Data is split repeatedly into leaves, which contain at most C training samples. Leaf RFMs are trained on the data at each leaf. (B) During inference, test data is routed to the appropriate leaf RFM based on split directions. The prediction is generated by the selected leaf RFM.

- (1) We tune over a more general class of kernels $K_{p,q}(x, x') = \exp(-\|x - x'\|_q^p / L^p)$ that are positive definite for $0 < p \leq q \leq 2$ [30, Theorems 1, 5]. In particular, we use either $q = 2$ (a generalized Laplace kernel) or $q = p$ (a product of 1D Laplace kernels).
- (2) We tune over using the full AGOP and just the diagonal of the AGOP. The latter is known to be a theoretically grounded approach for coordinate selection [38], and introduces an axis-aligned bias that has been observed to match the structure of tabular data [16].

In addition to the above changes, we also implemented optimizations to speed up computations for kernels with $q = 1$ on categorical variables and an adaptive approach for tuning bandwidth separately for data on each leaf. Additional details regarding these changes and hyperparameter search spaces for leaf RFMs on TALENT and Meta-test [19] are provided in Appendix A.

3.2 Tree-based data partitioning

We now explain how xRFM builds a binary tree structure to partition data into leaves on which leaf RFMs are trained. First, given a dataset S with n samples, we subsample m points and train a leaf RFM (referred to as a *split* model) for one iteration on this subsample. The purpose of this split model is to learn a direction that can be used to partition the data into two subsets. To this end, we extract the top eigenvector, v , of the AGOP from the split model and create two subsets of the n datapoints: $S_1 = \{x \in S ; v^T x > \text{Median}(v^T z \text{ for } z \in S)\}$ and $S_2 = \{x \in S ; v^T x \leq \text{Median}(v^T z \text{ for } z \in S)\}$. We repeat this procedure on S_1 and S_2 and their corresponding children until all leaves are less than a maximum leaf size C . We finally train a leaf RFM on each of these leaves. This procedure is illustrated in Fig. 1A and detailed in the ‘TreePartition’ procedure of Algorithm A.2.

Note that our splitting procedure results in leaves of equal sizes (because of the split based on median), unlike tree-based predictive models, which can result in uneven splits. We typically split large datasets until leaves contain at most 60,000 samples. Leaf RFM hyperparameters are tuned using only on the validation data that falls into the leaf (as determined by splits down the binary tree). In the case that validation data at a given leaf has too few samples, we further hold out a subset of the training data at the leaf to use for validation.

Note that it is possible to have split data based on unsupervised splitting procedures (e.g., those based on random projections or using top eigenvectors of PCA) [10]. A key advantage of our split approach is that it groups together data points based on the features most relevant for prediction, as is captured by the top eigenvector of the AGOP. We found that splitting in this manner outperformed splits based on unsupervised approaches, including those described above. Prior works have also split data using the random forest procedure. For example, the authors of Hollmann et al. [18] train TabPFN-v2 on the samples routed to a given leaf of a tree in a random forest. The procedure in xRFM differs as it stratifies samples by projection onto a direction rather than individual coordinates and produces only one balanced tree instead of a forest.

Advantages of tree splits over traditional methods for scaling kernels. Because of tree-based partitioning, xRFM is able to scale log-linearly in the number of samples during training¹ and logarithmically in the number of samples during inference. While this is a computationally appealing aspect in practice, we note that there are a number of existing methods for scaling kernel machines. Examples include the Nyström approximation [36] and fast preconditioner methods for solving kernel regression [2, 22, 23, 29].

A major advantage of xRFM over these other methods and kernel RFM itself is the ability for tree-based partitioning to learn features local to subsets of data. Here, in Fig. 2, we provide an example clearly demonstrating this benefit. In this example, the function $f : \mathbb{R}^d \rightarrow \mathbb{R}$ depends on coordinates x_1, x_3, x_5 if $x_0 > 0$ and depends on coordinates x_9, x_{11}, x_{13} if $x_0 \leq 0$. xRFM learns x_0 as the initial split direction (through the AGOP of the split model trained on a random subset), then learns the relevant features for each case in separate leaf RFM models. This decomposition is to be contrasted with that of running kernel RFM from [27] in which the model would simply return that $\{x_0, x_1, x_3, x_5, x_9, x_{11}, x_{13}\}$ are all relevant features without decomposing into the two cases.

4 xRFM performance

We now apply xRFM to two tabular data benchmarks: the TALENT benchmark [37] and large datasets from the meta-test benchmark [19]. We use the former to evaluate xRFM on datasets of various sizes between 500 and 100,000 training samples. We use the latter to evaluate xRFM on larger datasets with at least 70,000 samples (a setting in which direct linear solvers become intractable, taking more than 40GB VRAM).

Performance evaluation measures. When measuring performance on these datasets, we use Root Mean Square Error (RMSE) for regression tasks (as is used in TALENT), and we use classification error (1 - classification accuracy) for classification tasks. To measure performance on aggregate over a benchmark, we consider the following aggregation metrics on individual dataset performance measures: Shifted Geometric Mean, Arithmetic Mean, and Normalized Arithmetic Mean. All metrics are defined in Appendix A.

Results on the TALENT benchmark. The TALENT benchmark consists of 300 total datasets comparing 31 different supervised learning algorithms [37]. Among these 31 algorithms are strong, widely used predictive models including Gradient Boosted Decision Tree (GBDT) variants (like XGBoost, CatBoost, LightGBM), hyper-parameter optimized neural networks (RealMLP), and recent transformer-based foundation models (TabPFNv2). The TALENT benchmark consists of 100 regression tasks, 120 binary classification tasks, and 80 multiclass classification tasks. The number of training samples per task varies between 500 and 100,000 and each task contains at least 5 input variables.

¹The complexity for the applications of RFM itself scales only linearly, but splitting the data with the median at every tree node increases the complexity to $O(n \log n)$.

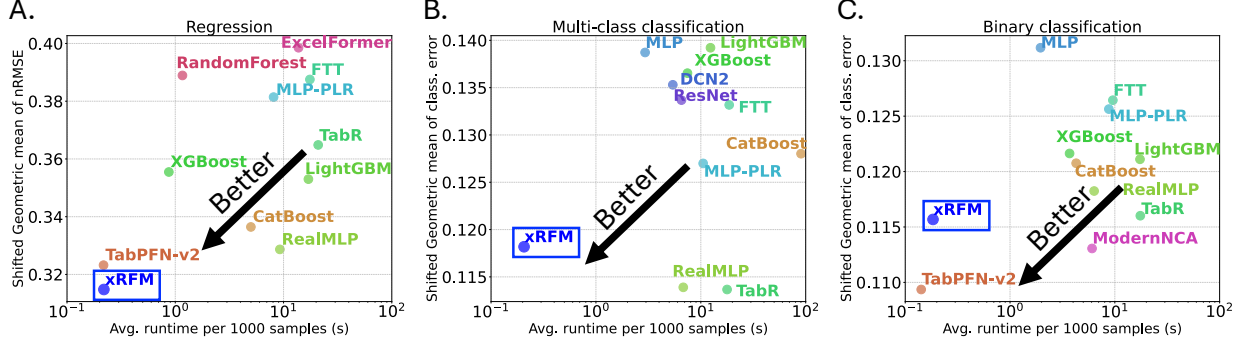


Figure 3: Performance and runtime of xRFM on the TALENT benchmark (500 to 100,000 training samples). The y-axis of each plot is the shifted geometric mean of the error across all datasets in that category, while the x-axis is the average over all datasets of the training plus inference time per 1000 samples (meaning if a dataset has n samples, we compute the training and inference time on the n samples divide the total time by $n/1000$). Note, that times do not include the time to tune hyperparameters. Also, TabPFN-v2 cannot run on more than 10k samples so performance and runtime on larger datasets is computed on a subsample (as was done in the TALENT benchmark). (A) nRMSE over 100 regression datasets, (B) classification error over 80 multi-class datasets, (C) classification error over 120 binary classification datasets.

xRFM is the best performing method on TALENT regression tasks according to all aggregation metrics over RMSEs on individual datasets (Fig. 3A). It is also the fastest method per configuration, although TabPFN-v2 does not incur a 100x overhead for hyperparameter tuning. xRFM is also competitive on classification datasets (Fig. 3B, C). Namely, xRFM is the third highest ranked method on classification tasks. We also compared xRFM performance against that of kernel ridge regression and standard RFM from [28]. We found xRFM was significantly better than these models (p -value $< 10^{-4}$, Wilcoxon test) (Fig. 4).

Additionally, we validated that the overall training+inference cost for xRFM scales linearly in the number of samples, making it a highly scalable tool in practice (Fig. 5). Notably, xRFM was extremely fast on small datasets: it was at least two orders of magnitude faster than other methods when the dataset contains fewer than 3000 samples (we omitted TabPFNv2 in our comparison as it could not be run on all datasets due to restrictions on the allowable sample size, number of features, and output dimensionality). An additional comparison on datasets up to 500k samples is presented in Fig. B.1.

Results on large datasets from the meta-test benchmark. To analyze xRFM performance on large datasets beyond those in TALENT, we considered the 17 largest datasets in the meta-test benchmark from [19] (Table B.6). These datasets contain between 70k and 500k samples (70k was near the limit, where linear solvers on 40GB VRAM GPUs become memory constrained).

We compared the performance of xRFM to other models with results reported in the literature on these 17 datasets (Fig. 6). These other models included GBDTs (XGBoost, LightGBM, CatBoost), and neural

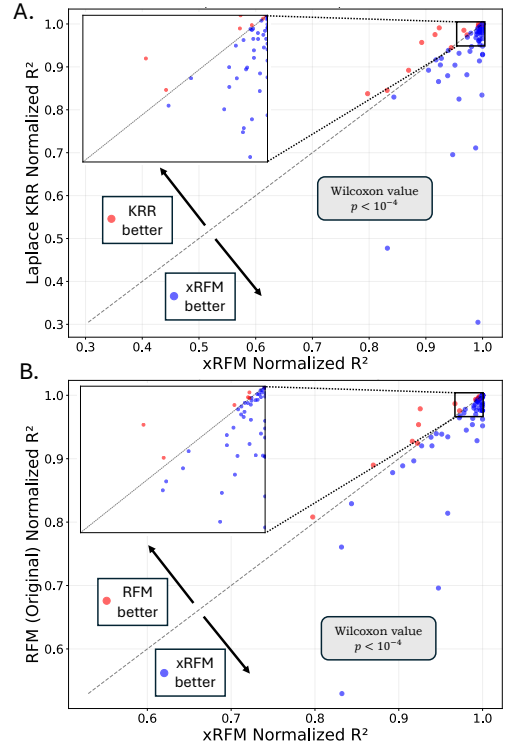


Figure 4: Comparisons of xRFM with (A) kernel ridge regression and (B) the original RFM [28] on TALENT regression datasets (performance metric is normalized R^2 A). Each point denotes a dataset.

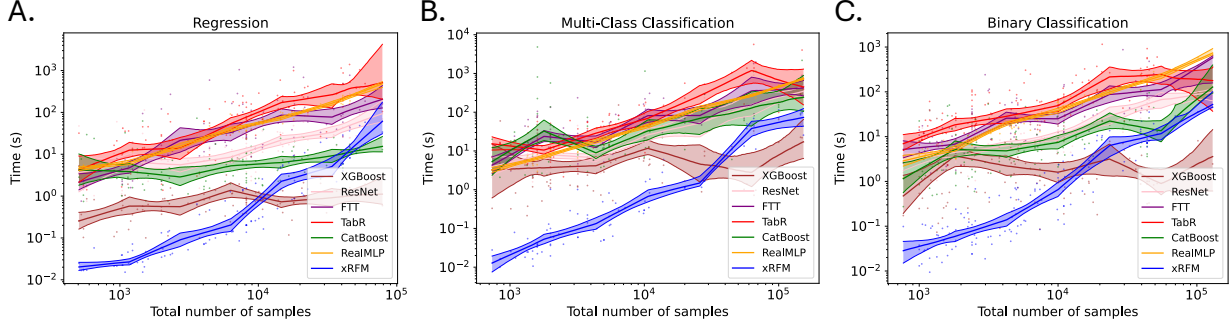


Figure 5: Total training and inference time for the best hyperparameter configuration as a function of the number of samples (training+validation+testing) across the TALENT benchmark. Curves indicate piecewise linear fit to measures on each dataset (shown as points). (A) Results across 100 regression tasks. (B) Results across 80 multi-class classification tasks. (C) Results across 120 binary classification tasks.

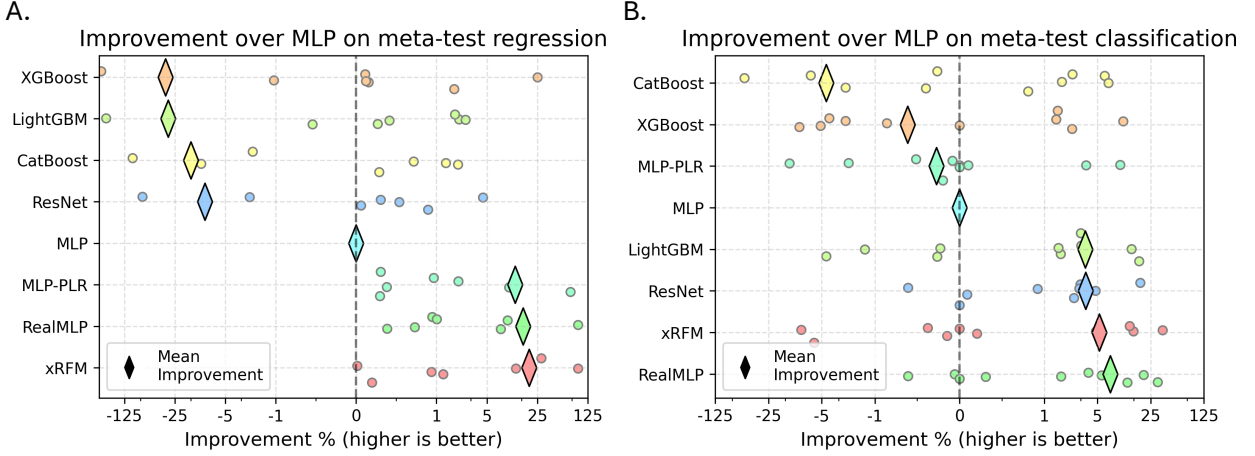


Figure 6: Performance comparison across 17 large datasets from meta-test (70,000–500,000 samples). (A, B) Percentage improvement over MLP error on (A) regression and (B) classification datasets. Average percentage improvement is denoted as a diamond. Points denote individual dataset results (points are jittered for visibility).

networks (ResNet, MLP, MLP-PLR [14], RealMLP). We reported percentage improvement of each method over MLPs (following the procedure in Gorishniy et al. [15], Qu et al. [26]). Similar to the results on TALENT, we found that xRFM was best on regression tasks, and second best on classification tasks. All results are presented in Tables B.6, B.7. For meta-test, we searched over slightly larger regularization parameters and slightly smaller bandwidth parameters to adapt to the much larger sample sizes of these datasets.

5 Features learned by xRFM on tabular data

An advantage of xRFM is that it immediately provides a means of identifying features relevant for prediction (without stacking on any additional interpretability methods). Namely, we can extract learned AGOPs of leaf RFMs and visualize the features they select.

We use two approaches for identifying features selected by the AGOP. The first is to identify the elements along the diagonal of the AGOP with highest magnitude. By definition, these entries indicate how much a leaf RFM’s predictions vary when perturbing a given coordinate. As such, they are a natural measure of feature importance. The second approach is to examine the loadings onto the top eigenvectors of the AGOP. This approach allows us to identify joint effects of feature perturbations on the prediction. Namely,

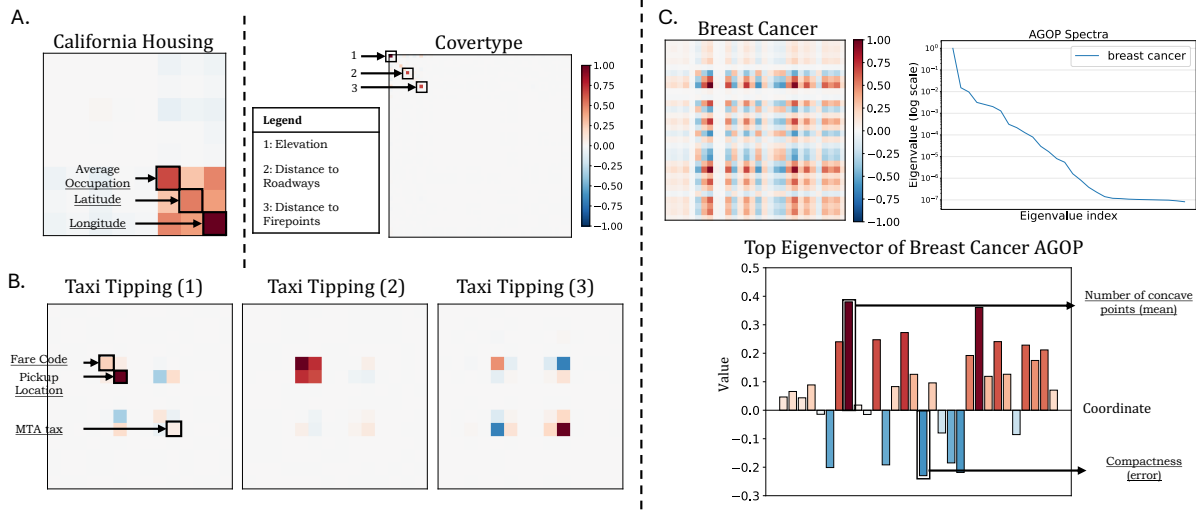


Figure 7: Interpreting xRFM through the AGOP of its constituent Leaf RFM models. (A) Examining the most important features for xRFM trained on California Housing (price prediction) and Covertype (dominant tree species prediction) datasets, based on the magnitude of diagonal entries. (B) Examining the features identified across three different Leaf RFM models for the NYC Taxi Tipping dataset. (C) Examining features learned for Breast Cancer detection from processed FNA imaging. The spectrum of this AGOP is plotted and the top eigenvector is shown in a bar plot. The most positive and negative entries of this eigenvector are boxed.

if coordinate i of the top eigenvector is positive and coordinate j is negative, then increasing one of these features and decreasing the other leads to a change in prediction.

We used both approaches above to understand what features were learned by xRFM on tabular data from TALENT and meta-test benchmarks (Fig. 7). As examples, we study the AGOPs for four such datasets:

- (1) California housing: a regression task for predicting the average price of a house.
- (2) Covertype: a multiclass classification task for identifying the dominant tree species in a given location.
- (3) NYC Taxi Tipping: a regression task for predicting the dollar tip amount in a taxi ride.
- (4) Breast cancer: a classification task for identifying malignancy from features of biopsy images.

As the California housing and breast cancer datasets contain fewer than 50k samples (the parameter we used for leaf size), we visualize a single AGOP. For covertype, we visualize one of the AGOPs from a leaf RFM (for this dataset, the leaf RFM AGOPs generally indicated the same pattern), and for taxi tipping we visualize several leaf RFM AGOPs. Upon visualization, it is apparent that AGOPs indicate low rank structure: either they highlight a subset of coordinates relevant for prediction (Fig. 7A, B) or they have a decay in the eigenvalue spectrum (Fig. 7C).

In Fig. 7A and B, we list feature names for the features with highest diagonal AGOP entries (darker shades of red indicate higher values). In all cases, we find that AGOP identified sensible features for prediction. For the California housing dataset, xRFM identified longitude, or east-west location, as the most important feature for predicting the average price of a house. Given that beach fronts (and major cities) in California are typically located to the west, the importance of house longitude is consistent with the hypothesis that homes closer to the beach are more expensive on average. For the Covertype prediction dataset, the example AGOP from a leaf RFM model showed that elevation, distance to roadways, and distance to firepoints were the most important features. This finding is consistent with the hypothesis that different elevations have different climates which significantly affect viability of tree species, and that fires / roadways can select for tree types that are fire-adapted or have avoided human logging. For the taxi tipping dataset, we observed that leaf RFMs identified varying local features. For example, one leaf RFM AGOP (denoted Taxi Tipping 1 in Fig. 7B) selected pickup location as an important feature, while this feature was less important for a

different leaf RFM AGOP (Taxi Tipping 3). Furthermore, fare code and the MTA tax have varying feature relationships at each leaf: in leaf RFM 1 and 2, the fare code and MTA tax had neutral or synergistic effects on the prediction value, while for leaf RFM 3, increasing fare code had the opposite effect on prediction as increasing MTA tax (shown as a blue square in Fig. 7B).

For the breast cancer dataset, the most important feature found by xRFM was the average number of concave points in the biopsy image, which has been shown to be a significant indicator of malignancy [25]. When examining the top eigenvector of the AGOP, we find that standard error in the compactness measurements of cell nuclei is the feature with highest importance that has an opposite effect on the malignancy label as concavity (Fig. 7C). This finding suggests that benign cells have less uniform compactness than malignant cells.

6 Discussion

Tabular data has historically provided a proving ground for the development of novel predictive models. However, even as the last years have seen spectacular improvements in language processing and computer vision, the progress in tabular data has been far more modest. While this may be changing with the developments such as hyperparameter-optimized neural networks (e.g., RealMLP [19]), and very recently, pre-trained transformer-based tabular networks, such as TabPFN-v2 [26], there is still large scope for improved tabular data prediction.

Kernel machines provide a powerful conceptually and computationally elegant approach for predictive modeling – one simply transforms data with a nonlinear feature map and then performs linear regression. Yet, historically, these methods have not out-performed Gradient Boosted Decision Trees (GBDTs), while also being significantly more difficult to scale. There are two key limitations of standard kernel machines: (1) standard kernel choices lack adaptivity to features relevant for prediction, and (1) naive implementations scale super-quadratically in the number of training samples, making them difficult to train on larger datasets (past 70k training samples). Significant progress in overcoming limitation (1) was made in recent work [27], which introduced Recursive Feature Machines (RFM) to enable feature learning in a range of models, including kernel machines. In fact, feature learning through RFM can be provably more sample efficient than standard kernels [38]. There has also been significant work addressing the limitation (2) including [23, 29, 36], to reference a few.

In this work, we have taken a different, tree-based approach to overcome these limitations. Our approach enables scalability to large datasets (log-linear training time and logarithmic inference time) while also leveraging the strength of RFM in identifying and exploiting local features. Indeed, the ability of xRFM to learn different features for different subpopulations of data through AGOPs at leaves is useful for characterizing heterogeneity across large datasets. Building on this core novelty and other algorithmic optimizations, we discuss a number of potential improvements and follow ups below.

A direction for future improvement of xRFM is to explore the use of iterative kernel solvers to train leaf RFMs. By using early stopping, these methods could obviate the need for tuning ridge regularization. The use of the adaptive binary tree structure to split data also opens up new avenues for exploration. For instance, it would be interesting to characterize the tradeoff between leaf size and performance and to develop new methods for determining when to stop splitting based statistics of leaf data. It might also be useful to consider alternative bandwidth selection methods for each leaf, for example by optimizing for bandwidths directly as in [17]. Lastly, it would be important to understand the effectiveness of AGOP as an interpretability mechanism, particularly in comparison to other widely used methods such as Shapley values [21], gradient-based importance scores [32, 33], and feature importance scores for tree-based models [6].

We also note that predictive modeling on tabular data is a highly active research area. There are continually new benchmarks and baselines, tuning, and cleaning methods to consider (e.g., using inner cross-validation, using metrics beyond accuracy for evaluating classification models, and studying weighted ensembles of models [11]). It is important to benchmark xRFM as such new settings arise.

Overall, we have shown that xRFM is an effective algorithm for inference from tabular data that scales to essentially unlimited data sizes and achieves performance exceeding or comparable to the current state-of-the-art. It combines the advantages of tree-based methods with the power and elegance of feature-learning kernel machines. We envision that xRFM will be used for both high-performing predictive modeling and uncovering heterogeneous structure in large-scale tabular data.

Acknowledgments

We would like to thank Jingang Qu, Ingo Steinwart, Tizian Wenzel, and Gaël Varoquaux for relevant discussions. We acknowledge support from the National Science Foundation (NSF) and the Simons Foundation for the Collaboration on the Theoretical Foundations of Deep Learning through awards DMS-2031883 and #814639 as well as the TILOS institute (NSF CCF-2112665), the Office of Naval Research (ONR N000142412631) and DARPA (HR001125CD020). This work used the programs (1) XSEDE (Extreme science and engineering discovery environment) which is supported by NSF grant numbers ACI-1548562, and (2) ACCESS (Advanced cyberinfrastructure coordination ecosystem: services & support) which is supported by NSF grants numbers #2138259, #2138286, #2138307, #2137603, and #2138296. Specifically, we used the resources from SDSC Expanse GPU compute nodes, and NCSA Delta system, via allocations TG-CIS220009.

References

- [1] E. Abbe, E. B. Adsera, and T. Misiakiewicz. The merged-staircase property: a necessary and nearly sufficient condition for sgd learning of sparse functions on two-layer neural networks. In P.-L. Loh and M. Raginsky, editors, *Proceedings of Thirty Fifth Conference on Learning Theory*, volume 178 of *Proceedings of Machine Learning Research*, pages 4782–4887. PMLR, 02–05 Jul 2022. URL <https://proceedings.mlr.press/v178/abbe22a.html>.
- [2] A. Abedsoltan, M. Belkin, and P. Pandit. Toward large kernel models. In *Proceedings of the 40th International Conference on Machine Learning*, ICML’23. JMLR.org, 2023.
- [3] N. Aronszajn. Theory of reproducing kernels. *Transactions of the American mathematical society*, 68(3):337–404, 1950.
- [4] D. Beaglehole, P. Súkeník, M. Mondelli, and M. Belkin. Average gradient outer product as a mechanism for deep neural collapse. In A. Globerson, L. Mackey, D. Belgrave, A. Fan, U. Paquet, J. Tomczak, and C. Zhang, editors, *Advances in Neural Information Processing Systems*, volume 37, pages 130764–130796. Curran Associates, Inc., 2024. URL https://proceedings.neurips.cc/paper_files/paper/2024/file/ec045a5ca2d8cf528591b4c34296370-Paper-Conference.pdf.
- [5] D. Beaglehole, A. Radhakrishnan, E. Boix-Adserà, and M. Belkin. Toward universal steering and monitoring of ai models, 2025. URL <https://arxiv.org/abs/2502.03708>.
- [6] L. Breiman, J. Friedman, R. A. Olshen, and C. J. Stone. *Classification and Regression Trees*. Chapman and Hall/CRC, 1st edition, 1984.
- [7] T. Chen and C. Guestrin. Xgboost: A scalable tree boosting system. In *Proceedings of the 22nd ACM SIGKDD international conference on knowledge discovery and data mining*, pages 785–794, 2016.
- [8] Y. Chen, E. N. Epperly, J. A. Tropp, and R. J. Webber. Randomly pivoted cholesky: Practical approximation of a kernel matrix with few entry evaluations. *Communications on Pure and Applied Mathematics*, 78(5):995–1041, 2025.
- [9] A. Damian, J. Lee, and M. Soltanolkotabi. Neural networks can learn representations with gradient descent. In P.-L. Loh and M. Raginsky, editors, *Proceedings of Thirty Fifth Conference on Learning Theory*, volume 178 of *Proceedings of Machine Learning Research*, pages 5413–5452. PMLR, 02–05 Jul 2022. URL <https://proceedings.mlr.press/v178/damian22a.html>.
- [10] S. Dasgupta and Y. Freund. Random projection trees and low dimensional manifolds. In *Proceedings of the fortieth annual ACM symposium on Theory of computing*, pages 537–546, 2008.
- [11] N. Erickson, L. Purucker, A. Tschalzev, D. Holzmüller, P. M. Desai, D. Salinas, and F. Hutter. Tabarena: A living benchmark for machine learning on tabular data. *arXiv preprint arXiv:2506.16791*, 2025.

[12] M. Fernández-Delgado, E. Cernadas, S. Barro, and D. Amorim. Do we need hundreds of classifiers to solve real world classification problems? *The Journal of Machine Learning Research*, 15(1):3133–3181, 2014.

[13] B. Ghorbani, S. Mei, T. Misiakiewicz, and A. Montanari. When do neural networks outperform kernel methods?*. *Journal of Statistical Mechanics: Theory and Experiment*, 2021(12):124009, Dec. 2021. ISSN 1742-5468. doi: 10.1088/1742-5468/ac3a81. URL <http://dx.doi.org/10.1088/1742-5468/ac3a81>.

[14] Y. Gorishniy, I. Rubachev, and A. Babenko. On embeddings for numerical features in tabular deep learning. *Advances in Neural Information Processing Systems*, 35:24991–25004, 2022.

[15] Y. Gorishniy, A. Kotelnikov, and A. Babenko. Tabm: Advancing tabular deep learning with parameter-efficient ensembling, 2025. URL <https://arxiv.org/abs/2410.24210>.

[16] L. Grinsztajn, E. Oyallon, and G. Varoquaux. Why do tree-based models still outperform deep learning on typical tabular data? In S. Koyejo, S. Mohamed, A. Agarwal, D. Belgrave, K. Cho, and A. Oh, editors, *Advances in Neural Information Processing Systems*, volume 35, pages 507–520. Curran Associates, Inc., 2022. URL https://proceedings.neurips.cc/paper_files/paper/2022/file/0378c7692da36807bdec87ab043cdadc-Paper-Datasets_and_Benchmarks.pdf.

[17] F. He, M. He, L. Shi, X. Huang, and J. A. K. Suykens. Enhancing kernel flexibility via learning asymmetric locally-adaptive kernels. *arXiv preprint arXiv:2310.05236*, 2023. URL <https://arxiv.org/abs/2310.05236>.

[18] N. Hollmann, S. Müller, L. Purucker, A. Krishnakumar, M. Körfer, S. B. Hoo, R. T. Schirrmeister, and F. Hutter. Accurate predictions on small data with a tabular foundation model. *Nature*, 637(8045):319–326, 2025.

[19] D. Holzmüller, L. Grinsztajn, and I. Steinwart. Better by default: Strong pre-tuned mlps and boosted trees on tabular data. *Advances in Neural Information Processing Systems*, 37:26577–26658, 2024.

[20] S. Kpotufe, A. Boulieras, T. Schultz, and K. Kim. Gradients weights improve regression and classification. *Journal of Machine Learning Research*, 17(22):1–34, 2016.

[21] S. M. Lundberg and S.-I. Lee. A unified approach to interpreting model predictions. *Advances in neural information processing systems*, 30, 2017.

[22] S. Ma and M. Belkin. Diving into the shallows: a computational perspective on large-scale shallow learning. *Advances in neural information processing systems*, 30, 2017.

[23] S. Ma and M. Belkin. Kernel machines that adapt to gpus for effective large batch training. *Proceedings of Machine Learning and Systems*, 1:360–373, 2019.

[24] N. Mallinar, D. Beaglehole, L. Zhu, A. Radhakrishnan, P. Pandit, and M. Belkin. Emergence in non-neural models: grokking modular arithmetic via average gradient outer product, 2024. URL <https://arxiv.org/abs/2407.20199>.

[25] A. Narasimha, B. Vasavi, and H. M. Kumar. Significance of nuclear morphometry in benign and malignant breast aspirates. *International Journal of Applied and Basic Medical Research*, 3(1):22–26, 2013.

[26] J. Qu, D. Holzmüller, G. Varoquaux, and M. L. Morvan. Tabicl: A tabular foundation model for in-context learning on large data. *arXiv preprint arXiv:2502.05564*, 2025.

[27] A. Radhakrishnan, D. Beaglehole, P. Pandit, and M. Belkin. Mechanism for feature learning in neural networks and backpropagation-free machine learning models. *Science*, 383(6690):1461–1467, 2024. doi: 10.1126/science.adi5639. URL <https://www.science.org/doi/abs/10.1126/science.adi5639>.

[28] A. Radhakrishnan, M. Belkin, and D. Drusvyatskiy. Linear recursive feature machines provably recover low-rank matrices. *Proceedings of the National Academy of Sciences*, 122(13):e2411325122, 2025. doi: 10.1073/pnas.2411325122. URL <https://www.pnas.org/doi/abs/10.1073/pnas.2411325122>.

[29] A. Rudi, L. Carratino, and L. Rosasco. Falkon: An optimal large scale kernel method. *Advances in neural information processing systems*, 30, 2017.

[30] I. J. Schoenberg. Positive definite functions on spheres. *Duke Mathematical Journal*, 9(1):96 – 108, 1942. doi: 10.1215/S0012-7094-42-00908-6. URL <https://doi.org/10.1215/S0012-7094-42-00908-6>.

[31] B. Schölkopf and A. J. Smola. *Learning with Kernels: Support Vector Machines, Regularization, Optimization, and Beyond*. MIT Press, 2002.

[32] R. R. Selvaraju, M. Cogswell, A. Das, R. Vedantam, D. Parikh, and D. Batra. Grad-cam: Visual explanations from deep networks via gradient-based localization. In *Proceedings of the IEEE international conference on computer vision*, pages 618–626, 2017.

[33] A. Shrikumar, P. Greenside, and A. Kundaje. Learning important features through propagating activation differences. In *International conference on machine learning*, pages 3145–3153. PMLR, 2017.

[34] S. Trivedi, J. Wang, S. Kpotufe, and G. Shakhnarovich. A consistent estimator of the expected gradient outerproduct. In *UAI*, pages 819–828, 2014.

[35] J. Vanschoren, J. N. van Rijn, B. Bischl, and L. Torgo. Openml: networked science in machine learning. *SIGKDD Explorations*, 15(2):49–60, 2013. doi: 10.1145/2641190.2641198. URL <http://doi.acm.org/10.1145/2641190.264119>.

[36] C. Williams and M. Seeger. Using the nyström method to speed up kernel machines. *Advances in neural information processing systems*, 13, 2000.

[37] H.-J. Ye, S.-Y. Liu, H.-R. Cai, Q.-L. Zhou, and D.-C. Zhan. A closer look at deep learning on tabular data. *arXiv preprint arXiv:2407.00956*, 2024.

[38] L. Zhu, D. Davis, D. Drusvyatskiy, and M. Fazel. Iteratively reweighted kernel machines efficiently learn sparse functions, 2025. URL <https://arxiv.org/abs/2505.08277>.

A Methods

A.1 Additional leaf-RFM modifications

Below, we provide further detail on the RFM modifications we made to implement leaf RFM.

- (1) We tune over a more general class of kernels $K_{p,q}(x, x') = \exp(-\|x - x'\|_q^p/L^p)$ that are positive definite for $0 < p \leq q \leq 2$ [30, Theorems 1, 5]. We typically search over $p \in \mathcal{U}(0.7, 1.4)$ and $q \in \{p, 2\}$ (Table A.1). In the case $q = p$, we obtain a kernel that is a product of 1D kernels and is therefore not rotation-invariant.
- (2) We tune over using the full AGOP and just the diagonal of the AGOP. The latter is known to be a theoretically grounded approach for coordinate selection [38], and introduces an axis-aligned bias that has been observed to match the structure of tabular data [16].

We also make the following changes to improve leaf RFM runtime on tabular data and to allow xRFM to adapt to the variance of input variables at each leaf:

- (3) We speed up computation for kernels with $q = 1$ on categorical variables taking c values by precomputing possible kernel entries as follows. We restrict the AGOP matrix to be block diagonal with a block for the $c \times c$ entries corresponding to the categorical variable. Letting $M_c \in \mathbb{R}^{c \times c}$ denote this block and $e_i \in \{0, 1\}^c$ denote the one-hot embedding of the categorical variable when it takes on value i , we precompute $M_c^{1/2}(e_i - e_j)$ for all $i, j \in [c]$.

(4) We tune over whether or not to use *adaptive bandwidth*, which involves separately scaling L at each leaf RFM by either $(\text{Median}(\|x - x'\|_1))^{-1}$ (if using product kernels) or $(\text{Median}(\|x - x'\|_2))^{-1}$ (if using orthogonally invariant kernels) for $x \neq x'$ at every leaf independently. Adaptive scaling allows xRFM to adapt to the variance of covariates at different leaves.

A.2 Metrics

Following [19], we report the shifted geometric mean of the error, which is the geometric mean of the error after shifting by a small value to prevent over-sensitivity to datasets with small errors. This metric is defined as follows.

Definition 1. *For a given set of errors on a benchmark $\varepsilon_1, \dots, \varepsilon_N$, the shifted geometric mean (SGM $_{\varepsilon}$) with parameter ε takes value:*

$$\text{SGM}_{\varepsilon} = \exp \left(\frac{1}{N} \sum_{i=1}^N \log(\varepsilon + \varepsilon_i) \right) .$$

In this work, as in Holzmüller et al. [19], we use $\varepsilon = 0.01$.

For regression tasks, we use normalized Root-mean-square-error (nRMSE), which is defined as follows.

Definition 2. *The normalized Root-mean-square-error is defined as,*

$$nRMSE = \sigma_y^{-1} \sqrt{\frac{1}{N} \sum_{i=1}^N (y_i - \hat{y}_i)^2}, \quad \text{where } \sigma_y = \sqrt{\frac{1}{N} \sum_{i=1}^N (y_i - \bar{y})^2}$$

When we refer to other normalized metrics, such as those used in Table B.1, Table B.2, Table B.3, Table B.4, Table B.5, we are min-max normalizing errors across methods for each dataset (see below).

Definition 3. *The normalized error \tilde{E}_j for method j on a given dataset, where the un-normalized error is E_j , has the form:*

$$\tilde{E}_j = \frac{E_j - E_{\min}}{E_{\max} - E_{\min}}, \quad E_{\min} = \min_k E_k, \quad E_{\max} = \max_k E_k .$$

A.3 Hyperparameters

Hyperparameter	TALENT	Meta-test
Bandwidth	$\log \mathcal{U}(1, 200)$	$\log \mathcal{U}(0.4, 80)$
Bandwidth Mode	{constant}	{constant, adaptive}
Categorical Transformations	{one_hot}	{ordinal_encoding, one_hot}
Diagonal	{False, True}	{False, True}
Early Stop Multiplier	1.06	1.05
Exponent p	$\mathcal{U}(0.7, 1.4)$	$\mathcal{U}(0.7, 1.3)$
Kernel Type	$\{K_{p,p}, K_{p,2}\}$	$\{K_{p,p}, K_{p,2}\}$
Normalization	{standard}	{standard}
Regularization	$\log \mathcal{U}(10^{-6}, 1)$	$\log \mathcal{U}(10^{-5}, 50)$
Refill size (N_{val})	1500	1500

Table A.1: Search spaces for xRFM on the TALENT (Figure 3) and Meta-test benchmarks (Figure 6).

Data pre-processing. For the TALENT benchmark, each method’s hyperparameters are tuned after fixing a single data normalization and categorical encoding scheme. For xRFM, kernel ridge regression, and standard kernel RFM, we one-hot encode categorical features and z-score input coordinates separately. For meta-test, methods also tune over choice of ordinal or one-hot encoding of categorical variables. On meta-test, we also normalize data by z-scoring input coordinates separately prior to tuning xRFM parameters.

Details of various methods. For scaling kernel ridge regression and the standard kernel RFM to large TALENT datasets, we used Eigenpro-2 (EP2) [23] that was initialized with the coefficients obtained from directly solving RFM on a random sample of 70,000 points. To tune the optimization hyperparameters for EP2, we tuned the model parameters for 100 trials on a random 70,000 sample subset, then for the final run, we used the tuned hyperparameters (and for kernel RFM the AGOP from the best iteration). For TabPFN-v2, we used the code provided from the benchmark github (<https://github.com/LAMDA-Tabular/TALENT>), which subsampled to 10,000 samples to avoid out-of-memory issues. The provided code did not apply TabPFN-v2 to datasets with more than 10 classes.

A.4 Algorithmic details

Note on AGOP computation For compute gradients of the predictor on training data (for AGOP computation), we omit the contribution to the gradient from the kernel evaluation between each training point and itself. This is because the kernel function is often not differentiable (for e.g. Laplace kernels) when evaluated for two identical points.

Algorithm A.1 Leaf RFM

Require:

- $x^{(1)}, \dots, x^{(n)} \in \mathbb{R}^d, y \in \mathbb{R}^{n \times c}$: Train data
- $X_{\text{val}} \in \mathbb{R}^{m \times d}, y_{\text{val}} \in \mathbb{R}^{m \times c}$: Validation data
- $K(\cdot, \cdot; L, p)$: Kernel parametrized by bandwidth $L \in \mathbb{R}^+$ and exponent $p \in (0, 2]$
- $\tau \in \mathbb{Z}^+$: Number of iterations
- $\lambda \in \mathbb{R}^+$: Ridge parameter
- $\varepsilon \in \mathbb{R}^+$: Stability parameter
- use_diag: Boolean indicating whether to use diagonal of AGOP only
- adapt_bandwidth: Boolean indicating whether to adapt bandwidth

```

 $M_0 \leftarrow I_{d \times d}$ 
 $X = [x^{(1)}, \dots, x^{(n)}]^\top \in \mathbb{R}^{n \times d}$ 
if adapt_bandwidth then
     $L \leftarrow \text{AdaptBandwidth}(L)$  ▷ Adapt bandwidth if enabled
end if
for  $t = 0, \dots, \tau - 1$  do
    if use_diag then
         $X_M \leftarrow X \odot \text{diag}(M)_t^{1/2}$ 
        Solve  $\alpha_t$  such that  $(K(X_M, X_M) + \lambda I)\alpha_t = y$ 
         $f^{(t)}(x) = K(x \odot \text{diag}(M)_t^{1/2}, X_M)\alpha_t$  ▷  $\odot$  denotes element-wise multiplication
    else
         $X_M \leftarrow X M_t^{1/2}$ 
        Solve  $\alpha_t$  such that  $(K(X_M, X_M) + \lambda I)\alpha_t = y$ 
         $f^{(t)}(x) = K(M_t^{1/2}x, X_M)\alpha_t$ 
    end if
    Compute  $E_t \leftarrow \text{Error}(f^{(t)}, X_{\text{val}}, y_{\text{val}})$  ▷ Validate model
     $M_{t+1} \leftarrow \frac{1}{n} \sum_{i=1}^n \nabla_x f^{(t)}(x^{(i)}) \nabla_x f^{(t)}(x^{(i)})^\top \in \mathbb{R}^{d \times d}$  ▷ Feature matrix (AGOP) computation
     $M_{t+1} \leftarrow M_{t+1} / (\varepsilon + \max_{i,j} M_{t+1}[i, j])$  ▷ Normalize feature matrix
end for
 $t^* \leftarrow \arg \min_t E_t$ 
return  $\alpha_{t^*}, M_{t^*}$  ▷ KRR coefficients:  $\alpha_{t^*}$ , feature matrix:  $M_{t^*}$  from best iteration on val. set

```

Algorithm A.2 TreePartition

Require:

- $\mathcal{D} = \{(x^{(1)}, y^{(1)}), \dots, (x^{(n)}, y^{(n)})\}$: Full dataset with $x^{(i)} \in \mathbb{R}^d, y^{(i)} \in \mathbb{R}^c$
- $K(\cdot, \cdot; L, p)$: Kernel parametrized by bandwidth $L \in \mathbb{R}^+$ and exponent $p \in (0, 2]$
- $N \in \mathbb{Z}^+$: Number of sample points for Leaf RFM
- $L \in \mathbb{Z}^+$: Maximum leaf size
- $\lambda \in \mathbb{R}^+$: Ridge parameter

function TREEPARTITION(\mathcal{D})

if $|\mathcal{D}| \leq L$ **then**

return Leaf node with dataset \mathcal{D}

end if

Sample N points $\mathcal{S} = \{(x^{(a_1)}, y^{(a_1)}), \dots, (x^{(a_N)}, y^{(a_N)})\}$ from \mathcal{D}

$X_s = [x^{(a_1)}, \dots, x^{(a_N)}]^\top \in \mathbb{R}^{N \times d}$

$y_s = [y^{(a_1)}, \dots, y^{(a_N)}]^\top \in \mathbb{R}^{N \times c}$

Solve α such that $(K(X_s, X_s) + \lambda I)\alpha = y$ ▷ Fit Leaf RFM on sampled data

Define predictor $f(x) = K(x, X_s)\alpha$

Compute AGOP: $M \leftarrow \frac{1}{N} \sum_{i=1}^N \nabla_x f(x^{(a_i)}) \nabla_x f(x^{(a_i)})^\top \in \mathbb{R}^{d \times d}$

Extract top eigenvector v_1 of M ▷ Principal direction

Project all data points: $p^{(i)} \leftarrow v_1^\top x^{(i)}$ for $i = 1, \dots, |\mathcal{D}|$

Compute median projection: $m \leftarrow \text{Median}(\{p^{(1)}, \dots, p^{(|\mathcal{D}|)}\})$

Split dataset:

$\mathcal{D}_{\text{left}} \leftarrow \{(x^{(i)}, y^{(i)}) \in \mathcal{D} : v_1^\top x^{(i)} \leq m\}$

$\mathcal{D}_{\text{right}} \leftarrow \{(x^{(i)}, y^{(i)}) \in \mathcal{D} : v_1^\top x^{(i)} > m\}$

$\text{left_child} \leftarrow \text{TreePartition}(\mathcal{D}_{\text{left}})$ ▷ Recursive call

$\text{right_child} \leftarrow \text{TreePartition}(\mathcal{D}_{\text{right}})$ ▷ Recursive call

return Internal node with splitting vector v_1 , threshold m , and children

end function

Algorithm A.3 Route (*find the leaf that contains a point*)

Require:

- \mathcal{T} : a (possibly trained) tree whose internal nodes store
 - splitting vector $v_1 \in \mathbb{R}^d$
 - threshold $m \in \mathbb{R}$
- $x \in \mathbb{R}^d$: query point

function ROUTE(x, \mathcal{T})

$r \leftarrow \mathcal{T}.\text{root}$ ▷ Initialize current node r from the tree

while r is an internal node **do**

if $v_1^\top x \leq r.\text{threshold}$ **then** ▷ Check if projection is less than (median) threshold

$r \leftarrow r.\text{left_child}$

else

$r \leftarrow r.\text{right_child}$

end if

end while

return r ▷ r is now the leaf node that contains x

end function

Algorithm A.4 xRFM (*training*)

Require:

- $\mathcal{D}_{\text{train}}, \mathcal{D}_{\text{val}}$: training and validation sets
- $K(\cdot, \cdot; L, p)$: kernel (bandwidth L , exponent p)
- $\text{TreeHyp} = \{N, L_{\max}, \lambda_{\text{split}}\}$: hyper-parameters for TREEPARTITION
- $\text{LeafHyp} = \{\tau, \lambda_{\text{leaf}}, \varepsilon, \text{use_diag}\}$: hyper-parameters for LEAFRFM
- \mathcal{A} : linear solver used inside LEAFRFM

```

function xRFM-FIT( $\mathcal{D}_{\text{train}}, \mathcal{D}_{\text{val}}$ )
   $\mathcal{T} \leftarrow \text{TREEPARTITION}(\mathcal{D}_{\text{train}}, K, \text{TreeHyp})$  ▷ Alg. A.2
  for all leaf node  $\ell \in \text{LEAVES}(\mathcal{T})$  do
     $\mathcal{D}_{\ell}^{\text{train}} \leftarrow$  data stored in  $\ell$ 
     $\mathcal{D}_{\ell}^{\text{val}} \leftarrow \{(x, y) \in \mathcal{D}_{\text{val}} : \text{ROUTE}(x, \mathcal{T}) = \ell\}$ 
     $(\alpha_{\ell}, M_{\ell}) \leftarrow \text{LEAFRFM}(\mathcal{D}_{\ell}^{\text{train}}, \mathcal{D}_{\ell}^{\text{val}}, K, \text{LeafHyp}, \mathcal{A})$  ▷ Alg. A.1
    Define predictor  $f_{\ell}(x)$  according to  $(\alpha_{\ell}, M_{\ell})$  and store it in  $\ell$ 
  end for
  return  $\mathcal{T}$  ▷ Tree whose leaves now carry trained predictors
end function

```

Algorithm A.5 xRFM (*inference*)

Require:

- \mathcal{T} : trained tree returned by xRFM-FIT (Alg. A.4)
- $x \in \mathbb{R}^d$: test point

```

function xRFM-PREDICT( $\mathcal{T}, x$ )
   $\ell \leftarrow \text{ROUTE}(x, \mathcal{T})$  ▷ Alg. A.3
   $\hat{y} \leftarrow f_{\ell}(x)$  ▷ Leaf predictor stored in  $\ell$ 
  return  $\hat{y}$ 
end function

```

B All results

Method	Rank	Score	Norm. Score	Top-1 (%)	Top-3 (%)	Top-5 (%)	Top-8 (%)	SGM_ϵ
xRFM	5.50	0.315	0.041	15.0	41.0	59.0	78.0	0.315
TabPFN-v2	6.46	0.323	0.066	23.0	45.0	61.0	72.0	0.323
CatBoost	7.67	0.336	0.052	9.00	25.0	43.0	69.0	0.336
RealMLP	8.14	0.329	0.075	7.00	22.0	38.0	62.0	0.329
ModernNCA	9.36	0.365	0.096	14.0	30.0	38.0	55.0	0.365
LightGBM	9.82	0.353	0.061	5.00	20.0	35.0	53.0	0.353
XGBoost	10.6	0.355	0.070	2.00	15.0	33.0	47.0	0.355
TabR	10.6	0.365	0.132	5.00	22.0	34.0	47.0	0.365
FTT	12.0	0.388	0.148	3.00	11.0	16.0	34.0	0.388
Laplace KRR	12.3	0.373	0.101	3.00	10.0	20.0	34.0	0.373
MLP-PLR	12.7	0.381	0.141	0.0	9.00	16.0	34.0	0.381
Excelformer	12.7	0.399	0.156	0.0	2.00	11.0	28.0	0.399
PTARL	13.1	0.390	0.113	3.00	6.00	8.00	19.0	0.390
RandomForest	13.3	0.389	0.087	5.00	14.0	22.0	35.0	0.389
AutoInt	14.3	0.399	0.157	1.00	2.00	7.00	13.0	0.399
Node	14.4	0.451	0.195	1.00	7.00	18.0	31.0	0.451
MLP	15.2	0.418	0.167	1.00	3.00	5.00	11.0	0.418
DCN2	15.2	0.473	0.227	0.0	2.00	9.00	20.0	0.473
ResNet	15.6	0.426	0.175	0.0	3.00	7.00	15.0	0.426
Tangos	16.3	0.432	0.173	0.0	2.00	4.00	10.0	0.432
SNN	17.1	0.419	0.174	0.0	2.00	4.00	8.00	0.419
kNN	19.1	0.459	0.189	2.00	4.00	5.00	11.0	0.459
TabNet	21.5	0.475	0.226	0.0	0.0	0.0	0.0	0.475
GrowNet	23.0	0.619	0.323	0.0	0.0	0.0	1.00	0.619
SVM	23.2	0.612	0.345	0.0	0.0	1.00	1.00	0.612
TabTransformer	26.4	1.07	0.750	1.00	1.00	2.00	3.00	1.07
SwitchTab	26.9	1.29	0.745	0.0	0.0	0.0	1.00	1.29
Danets	27.2	1.12	0.830	0.0	1.00	1.00	3.00	1.12

Table B.1: Full TALENT Regression results across 100 datasets. Rank is the average rank among the ordered methods over all datasets. Score is the metric we use to compare methods in Figure 3, in this case SGM_ϵ . Normalized score is the arithmetic mean of the normalized nRMSE. Top-X (%) is the percentage of datasets for which that method is in the top X ranks. The final column is the shifted geometric mean error (SGM_ϵ).

Method	Rank	Score	Norm. Score	Top-1 (%)	Top-3 (%)	Top-5 (%)	Top-8 (%)	SGM _ε
TabPFN-v2	7.04	0.823	0.935	26.5	51.5	61.8	70.6	0.108
xRFM	7.63	0.823	0.921	8.82	38.2	55.9	69.1	0.109
RealMLP	7.70	0.823	0.918	10.3	20.6	45.6	66.2	0.107
TabR	8.07	0.828	0.932	8.82	25.0	38.2	58.8	0.106
ModernNCA	8.90	0.825	0.913	10.3	29.4	42.6	60.3	0.106
CatBoost	10.3	0.819	0.906	1.47	19.1	38.2	51.5	0.117
LightGBM	11.7	0.813	0.883	5.88	20.6	30.9	44.1	0.125
XGBoost	12.2	0.815	0.887	4.41	17.6	26.5	41.2	0.124
ResNet	12.2	0.807	0.879	0.0	4.41	19.1	35.3	0.127
FTT	12.8	0.810	0.868	0.0	4.41	10.3	27.9	0.125
MLP-PLR	13.2	0.815	0.881	0.0	7.35	11.8	25.0	0.119
Laplace KRR	13.5	0.804	0.865	5.88	16.2	20.6	33.8	0.133
DCN2	14.0	0.806	0.865	1.47	5.88	10.3	27.9	0.127
MLP	14.2	0.805	0.864	0.0	5.88	8.82	19.1	0.131
SNN	14.9	0.805	0.858	0.0	0.0	2.94	8.82	0.129
AutoInt	15.7	0.804	0.858	0.0	0.0	1.47	8.82	0.130
RandomForest	15.8	0.797	0.832	5.88	8.82	11.8	26.5	0.137
Excelformer	16.1	0.805	0.854	0.0	0.0	5.88	17.6	0.127
Tangos	16.5	0.797	0.844	0.0	1.47	7.35	13.2	0.133
TabCaps	16.5	0.797	0.837	0.0	1.47	5.88	13.2	0.134
Danets	17.7	0.795	0.829	0.0	1.47	2.94	7.35	0.137
PTARL	19.0	0.796	0.808	0.0	0.0	1.47	4.41	0.139
kNN	20.1	0.786	0.773	4.41	7.35	10.3	14.7	0.152
LogReg	20.1	0.767	0.755	1.47	4.41	7.35	13.2	0.162
TabTransformer	21.5	0.771	0.739	0.0	1.47	1.47	4.41	0.155
Node	22.0	0.767	0.742	0.0	4.41	7.35	10.3	0.173
SVM	23.4	0.750	0.697	2.94	5.88	5.88	8.82	0.182
GrowNet	24.4	0.691	0.596	0.0	0.0	1.47	5.88	0.216
SwitchTab	25.0	0.748	0.674	0.0	1.47	1.47	1.47	0.187
TabNet	26.0	0.753	0.616	0.0	0.0	0.0	0.0	0.183
NaiveBayes	29.4	0.609	0.328	0.0	0.0	0.0	0.0	0.321
NCM	30.5	0.627	0.279	0.0	0.0	1.47	1.47	0.326

Table B.2: Full TALENT Multiclass classification (≤ 10 classes) results. Rank is the average rank among the ordered methods over all datasets. (Normalized) Score is the metric we use to compare methods in Figure 3. In this case score is the mean classification accuracy (1 minus the error in Figure 3). Top-X (%) is the percentage of datasets for which that method is in the top X ranks. The final column is the shifted geometric mean error (SGM_ε).

Method	Rank	Score	Norm. Score	Top-1 (%)	Top-3 (%)	Top-5 (%)	Top-8 (%)	SGM_ε
RealMLP	3.67	0.730	0.962	8.33	58.3	91.7	91.7	0.164
xRFM	6.08	0.716	0.941	25.0	25.0	66.7	75.0	0.185
TabR	6.08	0.720	0.945	8.33	50.0	50.0	66.7	0.172
ResNet	6.33	0.720	0.946	0.0	16.7	50.0	83.3	0.178
ModernNCA	6.75	0.713	0.911	33.3	41.7	50.0	83.3	0.168
FTT	8.79	0.709	0.917	0.0	8.33	25.0	50.0	0.187
MLP-PLR	8.79	0.712	0.923	0.0	0.0	25.0	50.0	0.185
MLP	9.58	0.710	0.919	0.0	0.0	8.33	41.7	0.190
Laplace KRR	10.8	0.679	0.887	0.0	16.7	41.7	50.0	0.218
DCN2	11.2	0.707	0.913	0.0	8.33	8.33	8.33	0.193
AutoInt	12.1	0.701	0.897	0.0	0.0	0.0	25.0	0.194
SNN	12.2	0.704	0.904	0.0	0.0	0.0	33.3	0.197
CatBoost	12.8	0.679	0.840	8.33	33.3	33.3	33.3	0.218
Danets	15.9	0.687	0.880	0.0	0.0	0.0	0.0	0.215
Tangos	16.0	0.660	0.820	8.33	8.33	8.33	16.7	0.225
XGBoost	16.2	0.678	0.872	8.33	8.33	8.33	25.0	0.236
Excelformer	16.5	0.675	0.849	0.0	0.0	0.0	16.7	0.217
TabCaps	16.8	0.670	0.851	0.0	0.0	0.0	0.0	0.231
LightGBM	16.9	0.668	0.848	0.0	0.0	0.0	16.7	0.261
PTARL	18.6	0.656	0.821	0.0	0.0	0.0	0.0	0.233
kNN	20.2	0.637	0.799	0.0	0.0	0.0	8.33	0.273
RandomForest	20.7	0.620	0.780	0.0	8.33	8.33	8.33	0.311
TabTransformer	20.8	0.582	0.700	0.0	0.0	8.33	8.33	0.307
LogReg	22.0	0.538	0.620	0.0	0.0	0.0	0.0	0.338
SVM	25.0	0.486	0.522	0.0	8.33	8.33	8.33	0.385
SwitchTab	25.2	0.525	0.602	0.0	0.0	0.0	0.0	0.372
Node	26.2	0.536	0.611	0.0	0.0	0.0	0.0	0.402
GrowNet	26.2	0.402	0.475	0.0	0.0	0.0	0.0	0.565
TabNet	26.3	0.486	0.516	0.0	0.0	0.0	0.0	0.368
NaiveBayes	29.5	0.410	0.378	0.0	0.0	0.0	0.0	0.545
NCM	30.2	0.399	0.338	0.0	0.0	0.0	0.0	0.552

Table B.3: Full TALENT Multiclass classification (> 10 classes) results. Rank is the average rank among the ordered methods over all datasets. (Normalized) Score is the metric we use to compare methods in Figure 3. In this case score is the mean classification accuracy (1 minus the error in Figure 3). Top-X (%) is the percentage of datasets for which that method is in the top X ranks. The final column is the shifted geometric mean error (SGM_ε).

Method	Rank	Score	Norm. Score	Top-1 (%)	Top-3 (%)	Top-5 (%)	Top-8 (%)	SGM _ε
RealMLP	7.26	0.839	0.952	7.41	14.8	33.3	74.1	0.125
TabR	7.72	0.844	0.971	18.5	33.3	55.6	70.4	0.116
xRFM	8.83	0.841	0.958	14.8	25.9	37.0	66.7	0.123
ModernNCA	9.50	0.843	0.965	3.70	33.3	44.4	59.3	0.120
CatBoost	9.93	0.827	0.892	11.1	29.6	37.0	55.6	0.128
LightGBM	10.2	0.826	0.886	7.41	25.9	44.4	55.6	0.128
TabPFN-v2	10.8	0.834	0.924	14.8	22.2	29.6	48.1	0.129
MLP-PLR	11.2	0.827	0.891	0.0	3.70	18.5	40.7	0.131
XGBoost	11.9	0.824	0.876	7.41	22.2	33.3	51.9	0.129
FTT	12.3	0.829	0.902	0.0	11.1	18.5	33.3	0.135
MLP	12.6	0.833	0.916	0.0	7.41	14.8	29.6	0.130
ResNet	13.1	0.834	0.921	0.0	7.41	7.41	29.6	0.130
DCN2	13.2	0.832	0.920	0.0	3.70	3.70	25.9	0.130
PTARL	13.3	0.831	0.912	0.0	3.70	11.1	14.8	0.131
AutoInt	13.6	0.831	0.912	0.0	0.0	3.70	14.8	0.130
Excelformer	14.6	0.821	0.859	3.70	7.41	7.41	11.1	0.143
SNN	14.6	0.831	0.913	0.0	3.70	7.41	18.5	0.131
Laplace KRR	17.0	0.826	0.881	3.70	11.1	14.8	18.5	0.138
Danets	17.3	0.827	0.889	0.0	0.0	0.0	0.0	0.133
TabCaps	18.4	0.822	0.863	0.0	3.70	7.41	7.41	0.136
TabTransformer	19.2	0.816	0.797	0.0	3.70	7.41	18.5	0.160
RandomForest	19.5	0.806	0.773	0.0	3.70	7.41	18.5	0.144
Node	20.1	0.793	0.725	3.70	3.70	3.70	7.41	0.151
LogReg	20.5	0.807	0.779	0.0	7.41	18.5	25.9	0.159
Tangos	20.7	0.811	0.799	0.0	0.0	3.70	3.70	0.139
SVM	21.8	0.802	0.755	0.0	0.0	3.70	18.5	0.162
GrowNet	22.6	0.804	0.772	0.0	0.0	0.0	3.70	0.160
TabNet	23.2	0.814	0.819	0.0	0.0	0.0	0.0	0.142
kNN	24.3	0.787	0.674	0.0	0.0	0.0	7.41	0.166
SwitchTab	27.3	0.786	0.671	0.0	0.0	0.0	0.0	0.163
NaiveBayes	30.2	0.678	0.154	0.0	0.0	0.0	0.0	0.283
NCM	31.3	0.679	0.174	0.0	0.0	0.0	0.0	0.281

Table B.4: Full TALENT Binary classification ($> 10,000$ samples) results. Rank is the average rank among the ordered methods over all datasets. (Normalized) Score is the metric we use to compare methods in Figure 3. In this case score is the mean classification accuracy (1 minus the error in Figure 3). Top-X (%) is the percentage of datasets for which that method is in the top X ranks. The final column is the shifted geometric mean error (SGM_ε).

Method	Rank	Score	Norm. Score	Top-1 (%)	Top-3 (%)	Top-5 (%)	Top-8 (%)	SGM _ε
TabPFN-v2	4.99	0.864	0.946	25.8	62.4	74.2	80.6	0.104
ModernNCA	10.2	0.856	0.886	14.0	21.5	33.3	51.6	0.111
CatBoost	10.2	0.845	0.867	5.38	23.7	35.5	55.9	0.119
LightGBM	10.3	0.845	0.869	6.45	19.4	35.5	55.9	0.119
TabR	10.4	0.851	0.872	4.30	14.0	30.1	44.1	0.116
xRFM	10.7	0.853	0.869	5.38	29.0	41.9	51.6	0.114
XGBoost	11.3	0.844	0.850	4.30	17.2	34.4	49.5	0.120
RealMLP	11.5	0.850	0.863	1.08	7.53	18.3	37.6	0.116
FTT	13.2	0.836	0.813	1.08	7.53	18.3	33.3	0.124
MLP-PLR	14.1	0.838	0.816	0.0	3.23	11.8	26.9	0.124
RandomForest	14.2	0.836	0.823	4.30	10.8	20.4	34.4	0.129
AutoInt	15.1	0.834	0.803	0.0	3.23	5.38	16.1	0.129
Tangos	15.3	0.834	0.799	0.0	2.15	7.53	18.3	0.131
DCN2	15.5	0.839	0.815	1.08	2.15	9.68	21.5	0.127
Laplace KRR	15.6	0.836	0.800	2.15	15.1	20.4	26.9	0.133
MLP	15.9	0.836	0.796	1.08	3.23	8.60	17.2	0.132
ResNet	16.0	0.839	0.810	1.08	3.23	8.60	17.2	0.129
TabCaps	16.1	0.835	0.804	1.08	3.23	6.45	14.0	0.130
Excelformer	16.5	0.830	0.778	0.0	1.08	7.53	19.4	0.131
SNN	16.6	0.836	0.800	1.08	3.23	4.30	6.45	0.129
Node	16.9	0.824	0.756	0.0	6.45	15.1	25.8	0.137
PTARL	16.9	0.830	0.779	0.0	1.08	3.23	7.53	0.134
Danets	17.9	0.829	0.758	0.0	3.23	7.53	15.1	0.137
TabTransformer	19.7	0.820	0.714	1.08	1.08	7.53	12.9	0.148
LogReg	20.1	0.819	0.723	3.23	7.53	12.9	18.3	0.146
kNN	20.8	0.811	0.677	5.38	9.68	14.0	18.3	0.158
SVM	21.5	0.816	0.697	2.15	4.30	6.45	11.8	0.150
GrowNet	22.1	0.817	0.713	0.0	0.0	0.0	2.15	0.151
SwitchTab	23.9	0.809	0.675	0.0	0.0	0.0	1.08	0.156
TabNet	25.8	0.802	0.633	0.0	0.0	0.0	0.0	0.157
NaiveBayes	28.6	0.695	0.280	1.08	3.23	3.23	4.30	0.253
NCM	29.9	0.723	0.231	0.0	0.0	1.08	2.15	0.257

Table B.5: Full TALENT Binary classification ($\leq 10,000$ samples) results. Rank is the average rank among the ordered methods over all datasets. (Normalized) Score is the metric we use to compare methods in Figure 3. In this case score is the mean classification accuracy (1 minus the error in Figure 3). Top-X (%) is the percentage of datasets for which that method is in the top X ranks. The final column is the shifted geometric mean error (SGM_ε).

Dataset	xRFM	XGB	CatBoost	LGBM	RealMLP	MLP-PLR	MLP	ResNet
Airlines.DepDelay.10M	0.9823	0.9813	0.9796	0.9798	0.9786	0.9795	0.9824	0.9818
Allstate.Claims.Severity	0.6544	0.6547	0.6510	0.6530	0.6495	0.6537	0.6557	0.6537
black.friday	0.6864	0.6807	0.6792	0.6787	0.6859	0.6862	0.6929	0.6892
Buzzinsocialmedia.Twitter	0.2035	0.2134	0.3147	0.2789	0.2566	0.2553	0.2840	0.2906
nyc-taxi-green-dec-2016	0.5817	0.6649	0.6567	0.6489	0.6142	0.6523	0.6657	0.6365
wave_energy	0.0022	0.0918	0.0499	0.0821	0.0024	0.0073	0.0254	0.0434
Yolanda	0.7829	0.8012	0.8094	0.7970	0.7869	0.7897	0.7927	0.7856

Table B.6: Meta-test regression datasets with more than 70,000 samples. Error reported is nRMSE averaged over five train/test splits using `pytabkit`.

Dataset	xRFM	XGB	CatBoost	LGBM	RealMLP	MLP-PLR	MLP	ResNet
airlines	0.3347	0.3292	0.3315	0.3287	0.3344	0.3342	0.3342	0.3339
covertype	0.0259	0.0420	0.0612	0.0333	0.0280	0.0364	0.0404	0.0385
Higgs	0.2674	0.2576	0.2576	0.2549	0.2473	0.2528	0.2515	0.2435
jannis	0.2729	0.2799	0.2816	0.2779	0.2702	0.2764	0.2865	0.2795
MiniBooNE	0.0550	0.0529	0.0538	0.0525	0.0484	0.0504	0.0503	0.0488
numerai28.6	0.4789	0.4812	0.4790	0.4782	0.4800	0.4775	0.4771	0.4800
porto-seguro	0.0380	0.0380	0.0381	0.0381	0.0380	0.0380	0.0380	0.0380
dionis	0.0945	0.1219	0.1041	0.1076	0.0887	0.1257	0.1110	0.0907
Fashion-MNIST	0.0904	0.0928	0.0969	0.0895	0.0913	0.1064	0.1041	0.1011
kick	0.0977	0.0965	0.0956	0.0964	0.0976	0.0978	0.0979	0.0970

Table B.7: Meta-test classification datasets with greater than 70,000 samples. Error reported is classification error averaged over five train/test splits using `pytabkit`.

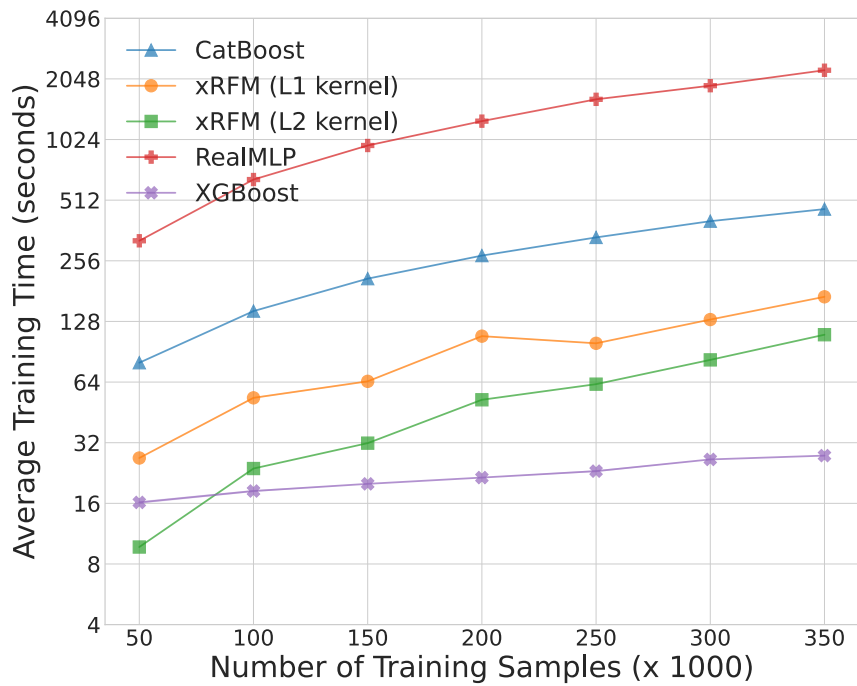


Figure B.1: Runtime comparison as a function of the number of training samples on the covtype dataset.